

# Optical absorption in undoped yttrium aluminum garnet

M. E. Innocenzi and R. T. Swimm

Department of Electrical Engineering and Center for Laser Studies, University of Southern California, Los Angeles, California 90089-1112

M. Bass

Department of Electrical Engineering and Physics and the Center for Research on Electrooptics and Lasers, University of Central Florida, Orlando, Florida 32816-0150

R. H. French

E. I. du Pont De Nemours & Company, Inc., Wilmington, Delaware 19880

M. R. Kokta

Union Carbide Crystal Products Division, Washougal, Washington 98671

(Received 23 January 1990; accepted for publication 10 April 1990)

Room-temperature optical absorption over a large dynamic range is reported for single-crystal undoped yttrium aluminum garnet ( $\text{Y}_3\text{Al}_5\text{O}_{12}$  or YAG). Absorption results are presented for the energy ranges 1.8 to 3.0 and 4.5 to 6.5 eV. For this work, ultraviolet (UV) absorption measurements were performed on four different boules of Czochralski-grown undoped YAG. Absorption features were observed at 4.8 and 5.6 eV which can be attributed, at least in part, to trace impurity concentrations. Along with the UV measurements, calorimetric absorption results are presented at several laser wavelengths in the visible and near infrared (IR). The calorimetric results suggest a value of  $1.5 \times 10^{-3} \text{ cm}^{-1}$  for the absorption coefficient of undoped YAG in the red and near IR. From the combination of UV and calorimetric measurements, an empirical estimate of the absorption coefficient from the visible to the UV is presented for undoped YAG. In addition to the absorption spectra, detailed chemical analyses and sample histories are given for the as-grown optical quality YAG utilized herein.

## I. INTRODUCTION

Yttrium aluminum garnet ( $\text{Y}_3\text{Al}_5\text{O}_{12}$  or YAG) was first synthesized by Yoder and Keith.<sup>1</sup> Single-crystal YAG is a clear, hard (8.5 on the Mohs scale)<sup>2</sup> cubic crystal of space group  $O_h^{10}$  ( $\text{Ia}3d$ ).<sup>3</sup> Since the work of Geusic, Morcos, and Van Uitert,<sup>4,5</sup> it has commonly been employed as a laser host for the rare-earth element Nd, but has been doped with transition metals and every element of the lanthanide series with the exception of Lu. In addition, YAG has been utilized as a color phosphor (Ce:YAG) for cathode ray tubes.<sup>5,6</sup>

Absorption results in the transparency region of single-crystal undoped YAG are limited primarily to the ultraviolet (UV). Early absorption results on undoped YAG were presented by O'Bryan and O'Connor.<sup>7</sup> O'Bryan and O'Connor grew YAG and other rare-earth garnets by the floating zone technique. Their UV spectra lacks detail and is limited to one piece of floating zone YAG. Another piece of early work was performed by Bass and Paldino.<sup>8</sup> They studied absorption bands that accrued from color center formation in undoped YAG. The first reasonably comprehensive work to appear was that of Slack *et al.*<sup>9</sup> on Czochralski (Cz)-grown undoped YAG, and was one of the few studies that supplied detailed growth information. Some chemical analysis (source unknown) was done on Slack's YAG crystals, but the results are not sample specific. Rooze and Anisimov<sup>10</sup> also reported UV absorption studies on undoped YAG. Their material was Cz grown, but no purities or growth information is given. Another

notable absorption study on undoped YAG was done by Wong, Rotman, and Warde,<sup>11</sup> in conjunction with optical studies on Ce:YAG crystals. Wong and co-workers' undoped YAG and Ce:YAG were grown at Airtron Corporation, but no impurity analysis was reported for the YAG samples utilized in the study. Other work on undoped YAG was performed by Tomiki *et al.*<sup>12,13</sup> and Devor, Pastor, and DeShazer.<sup>14</sup> Tomiki's absorption results consist of two UV spectra. No information is given as to purity or growth conditions of the samples. Devor and co-workers' research entails the identification of hydroxyl impurities and their effects. A large thrust is toward elimination of this type of impurity with postgrowth processing. Devor and co-workers performed a limited amount of emission spectroscopy to acquire impurity information on their YAG samples.

In reviewing the literature dealing with optical absorption in the transmissive region of undoped YAG, a complete study (i.e., one with a detailed growth, and chemical history) on high-quality YAG does not emerge. The current work represents such a study and presents detailed results that are representative of as-grown optical quality undoped YAG.

## II. EXPERIMENT

For this work, two different types of experimental studies were performed. In the UV, relative transmission was performed on samples of differing length to acquire the absorption coefficients. The UV spectroscopy required for

TABLE I. Additional growth parameters for YAG I-III.

| Growth parameters     |                |
|-----------------------|----------------|
| melt composition      | stoichiometric |
| orientation           | [1,1,1]        |
| pull rate             | 0.015 in./hr.  |
| rotation rate         | 15 rpm         |
| crucible              | Iridium        |
| temperature (at seed) | 1972-1976 °C   |

this work was performed on a McPherson 225 1-m vacuum monochromator. This apparatus has previously been described.<sup>15,16</sup> The maximum entrance and exit slit widths were 65 μm and the reproducibility of the scan drive was ± 1.5 Å. The MgF<sub>2</sub>-coated Al grating had 1200 lines/mm ruling and a blaze wavelength of 1500 Å. In the visible and near infrared (IR), laser calorimetry was utilized to obtain the absorption coefficient of the YAG. The calorimetric measurements were performed with several lasers and one calorimeter. The details of the experimental setup and the data analysis method have been published elsewhere.<sup>15,16</sup>

### III. SAMPLE HISTORY

For this work, four boules of undoped YAG were acquired and processed. To facilitate bookkeeping, the boules

are designated YAGs I-IV. All four boules are single-crystal Cz-grown Union Carbide material. The boules were free of coloration and twinning. The growth atmosphere was N<sub>2</sub> + 800 ppm O<sub>2</sub> (by volume) for YAGs II and III. For YAG I, it was strictly N<sub>2</sub>. The remainder of the growth parameters were identical for YAGs I, II, and III. They are listed in Table I. All material was as-grown with no after growth annealing. YAG IV was obtained several years ago and the specifics of the growth are not known. It was billed as standard undoped 4 9's purity YAG. YAG I and YAG II were grown with 5 9's purity Y<sub>2</sub>O<sub>3</sub> powder and 4 9's purity Al<sub>2</sub>O<sub>3</sub> powder. YAG III was grown with 5 9's purity Y<sub>2</sub>O<sub>3</sub> powder and 8 9's purity Al<sub>2</sub>O<sub>3</sub> powder. (All purities are the purported purities of the starting materials as stated by the material supplier.)<sup>17</sup> Impurity analyses were performed on YAGs I-IV by Northern Analytical Laboratory<sup>18</sup> using spark source mass spectrography (SSMS). The results of the impurity analyses are tabulated in Table II. Subsequent to the completion of the SSMS analyses of Table II, higher resolution SSMS analyses were performed on YAGs II and IV. These results are tabulated in Table III. In addition to increased sensitivity, the higher resolution analysis also helps eliminate interferences by clusters of atoms of the same atomic weight. Comparing the impurity analyses for YAGs II and IV from Tables II and III, it is seen that there are differences among the

TABLE II. Results of the YAG chemical analysis. Impurity concentrations are in ppmw and ppma. The former is a ratio of the atomic weight of the impurity to the average atomic weight of YAG and the latter is the number of impurity atoms per million atoms of YAG. The < and < signs are present at the detection limits and where possible interference from clusters of the same weight may have occurred. Elements not reported are less than 0.02 ppma nominal, which is the detection limit for these analyses. Generally, for elements with more than one isotope, the ppma nominal is corrected by the abundance factor for the most abundant isotope. As an example, for Nd, the detection limit becomes 0.08 ppma, i.e., 0.02 ppma nominal × (1.0/0.272), where 0.272 is the isotropic abundance of Nd<sup>142</sup>.

| Name | Concentration in ppmw |        |         |        | Concentration in ppma |        |         |        |
|------|-----------------------|--------|---------|--------|-----------------------|--------|---------|--------|
|      | YAG I                 | YAG II | YAG III | YAG IV | YAG I                 | YAG II | YAG III | YAG IV |
| F    | 0.1                   | 0.1    | 0.1     | 0.1    | 0.2                   | 0.2    | 0.2     | 0.2    |
| Na   | 0.6                   | 0.4    | 0.8     | 0.4    | 0.8                   | 0.5    | 1.0     | 0.5    |
| Mg   | <2                    | <2     | <2      | <2     | <2                    | <2     | <2      | <2     |
| Si   | <4                    | <4     | <4      | <4     | <4                    | <4     | <4      | <4     |
| P    | 0.05                  | 0.05   | 0.05    | 0.03   | 0.05                  | 0.05   | 0.05    | 0.03   |
| S    | <2                    | <2     | <2      | <2     | <2                    | <2     | <2      | <2     |
| Cl   | 10                    | 4      | 4       | 2      | 8                     | 3      | 3       | 2      |
| K    | 0.1                   | 0.04   | 0.09    | 0.04   | 0.08                  | 0.03   | 0.07    | 0.03   |
| Ca   | 4                     | 0.8    | 3       | 0.8    | 3                     | 0.6    | 2       | 0.6    |
| V    | <0.3                  | <0.3   | <0.3    | <0.3   | <0.2                  | <0.2   | <0.2    | <0.2   |
| Cr   | 0.3                   | 0.1    | 0.7     | 0.05   | 0.2                   | 0.07   | 0.4     | 0.03   |
| Mn   | 0.05                  | ...    | 0.05    | ...    | 0.03                  | ...    | 0.03    | ...    |
| Fe   | 4                     | 0.4    | 4       | 0.2    | 2                     | 0.2    | 2       | 0.1    |
| Ni   | 0.1                   | 0.08   | 0.1     | ...    | 0.07                  | 0.04   | 0.05    | ...    |
| Cu   | <0.2                  | <0.2   | <0.2    | <0.2   | <0.1                  | <0.1   | <0.1    | <0.1   |
| Ga   | 2                     | 0.2    | 0.4     | 2      | 1                     | 0.1    | 0.2     | 1      |
| Zr   | 0.9                   | <0.3   | 2       | <0.3   | 0.3                   | <0.1   | 0.5     | <0.1   |
| Ba   | <0.9                  | <0.9   | <0.9    | <0.9   | <0.2                  | <0.2   | <0.2    | <0.2   |
| La   | 0.1                   | <0.09  | 0.1     | <0.09  | 0.03                  | <0.02  | 0.03    | <0.02  |
| Ce   | <3                    | <3     | <3      | <3     | <0.7                  | <0.7   | <0.7    | <0.7   |
| Pr   | 0.1                   | <0.09  | 0.1     | <0.09  | 0.03                  | <0.02  | 0.03    | <0.02  |
| Nd   | 0.5                   | <0.4   | 0.5     | 0.5    | 0.1                   | <0.08  | 0.1     | 0.1    |
| Eu   | 0.3                   | ...    | ...     | ...    | 0.06                  | ...    | ...     | ...    |
| Gd   | 1                     | ...    | 0.5     | ...    | 0.2                   | ...    | 0.1     | ...    |
| Tb   | ...                   | 0.2    | ...     | ...    | ...                   | 0.03   | ...     | ...    |
| Dy   | 0.5                   | ...    | ...     | ...    | 0.1                   | ...    | ...     | ...    |
| Ho   | <0.2                  | 0.6    | <0.2    | 0.6    | <0.03                 | 0.1    | <0.03   | 0.1    |

TABLE III. Results of the higher sensitivity SSMS analyses performed on YAGs II and IV. These are longer duration analyses with increased sensitivity to 0.007 ppm nominal. In this analysis, the detection limit for Nd becomes 0.03 ppm or 0.1 ppmw. All analyses were performed by Northern Analytical Laboratory.

| Name | ppmw   |        | ppma   |        |
|------|--------|--------|--------|--------|
|      | YAG II | YAG IV | YAG II | YAG IV |
| B    | 0.06   | 0.06   | 0.2    | 0.2    |
| F    | 0.1    | 0.05   | 0.2    | 0.1    |
| Na   | 0.2    | 0.3    | 0.3    | 0.4    |
| Mg   | 1      | 1      | 2      | 2      |
| Si   | 2      | 2      | 2      | 2      |
| P    | 0.03   | 0.03   | 0.03   | 0.03   |
| S    | 2      | 1      | 2      | 1      |
| Cl   | 3      | 3      | 3      | 3      |
| K    | 0.2    | 0.2    | 0.2    | 0.2    |
| Ca   | 0.6    | 0.8    | 0.5    | 0.7    |
| V    | <0.1   | <0.1   | <0.07  | <0.07  |
| Cr   | 0.05   | 0.07   | 0.03   | 0.05   |
| Mn   | 0.02   | 0.01   | 0.01   | 0.007  |
| Fe   | 0.1    | 0.3    | 0.07   | 0.2    |
| Co   | <0.01  | <0.01  | <0.007 | <0.007 |
| Ni   | 0.02   | 0.02   | 0.01   | 0.01   |
| Cu   | 0.04   | 0.02   | 0.02   | 0.01   |
| Zn   | 0.04   | <0.02  | 0.02   | <0.01  |
| Ga   | 0.1    | 1      | 0.05   | 0.5    |
| Zr   | <0.1   | <0.1   | <0.04  | <0.04  |
| Ba   | <0.3   | <0.3   | <0.09  | <0.09  |
| La   | ...    | ...    | ...    | ...    |
| Ce   | <0.3   | <0.3   | <0.07  | <0.07  |
| Pr   | ...    | ...    | ...    | ...    |
| Nd   | ...    | ...    | ...    | ...    |
| Tb   | <0.05  | <0.05  | <0.01  | <0.01  |
| Dy   | 0.2    | <0.1   | 0.04   | <0.03  |
| Ho   | 0.1    | 0.05   | 0.02   | 0.01   |

results. Other than changes in the estimated concentrations of the impurities, new impurities appear in Table III (B, Co, Zn, Tb) while others (La, Pr, Nd) disappear. From the results of Table II, all of the YAG samples appear to be 4 9's purity while Table III suggests that YAGs II and IV may be 5 9's purity.

The YAG I-III boules were cut into 0.5-in.-diam cylinders of differing length. These were sent to Laser Power Optics<sup>19</sup> (LPO) for polishing where they received a high-quality chemical polish, the details being an LPO secret. YAG IV already existed in rectangularly shaped samples of differing length. These samples were cut and polished at The Aerospace Corporation.<sup>20</sup> The polishing technique was a standard mechanical method employing diamond paste. The smallest grit size was 1  $\mu\text{m}$ . This resulted in a coarser finish than that achieved on YAGs I-III.

#### IV. RESULTS AND DISCUSSION

A qualitative scattering test utilizing Kr<sup>+</sup> and Ar<sup>+</sup> ion lasers as probes was conducted on the YAG samples to determine whether they contained internal scattering centers. For YAG II and IV, no scattering was detected. However, upon examination of YAG I, a distinct filament of internal scattering centers was discernable along the laser

beam path. YAG III also showed some signs of internal scattering, but less than YAG I.

Although YAGs II and IV did not scatter the laser light, a distinct yellow-green luminescence emanated from these samples for probe wavelengths in the blue and violet. This phenomenon was also present in YAG III. This yellow-green luminescence appeared quite similar to that reported by Bernhardt.<sup>21</sup> The luminescence was excited in the 400- to 500-nm range, although no absorption was detectable on spectrophotometer scans in this region. The luminescent emission occurred from 500 to 660 nm and was broadly peaked in the 540- to 580-nm range. Bernhardt suggested the possibility that the luminescence could be related to the presence of Fe<sup>3+</sup> and Mn<sup>2+</sup>. Based on the current chemical analyses, Bernhardt's suggestion cannot be ignored because of the presence of Fe and Mn in YAGs II, III, and IV, although Mn was detected close to, or at, the sensitivity limit in all of the analyses. Another possible explanation for the yellow-green luminescence is the presence of Ce in the samples. Ce:YAG is known to emit yellow-green luminescence over the 500- to 660-nm range, and this Ce<sup>3+</sup> (5D to 4F) emission is also excited with 400- to 500-nm light.<sup>5,11</sup> Yellow-green Ce emission has been studied as a function of the partial pressure of oxygen in the annealing atmospheres of annealed Ce:YAG crystals. In cathode luminescence experiments, Robbins *et al.*<sup>22</sup> found that the yellow-green Ce luminescence decreased for Ce:YAG crystals annealed in oxidizing atmospheres. Also, Rotman and Warde<sup>23</sup> observed increased yellow-green Ce emission in photoluminescence studies for decreasing oxygen partial pressures in the annealing atmospheres of their Ce:YAG. The yellow-green Ce emission appears to be influenced by an intrinsic lattice defect associated with electrons trapped at oxygen vacancies.<sup>23-25</sup> Although annealing studies were not performed in the present study, we have observed that the yellow-green luminescence exhibited by undoped YAG is dependent upon the partial pressure of oxygen in the growth atmosphere, something which was not considered in the previous studies. As an example, YAG I, which was grown in the absence of O<sub>2</sub>, did not luminesce yellow-green although it contained Ce. The lack of yellow-green luminescence may have resulted from the reduction of the normally present Ce<sup>3+</sup> to Ce<sup>2+</sup>. However, in intentionally doped Ce:YAG crystals (0.4 wt. %), we have observed that the introduction of oxygen into the growth atmosphere decreases the efficiency of the Ce yellow-green luminescence. Obviously, the effect of oxygen atmospheres on the yellow-green luminescence is a complicated issue most likely involving Ce concentration, oxygen vacancies, and other background impurity concentrations. Additional studies with detailed chemical analyses will be required to elucidate the various dependencies involved.

As a second diagnostic, all of the YAG samples were scanned on a spectrophotometer before and after the UV absorption measurements. This was done to ensure that no additional absorptions occurred in the near IR, visible, or UV which would indicate color center formation in the

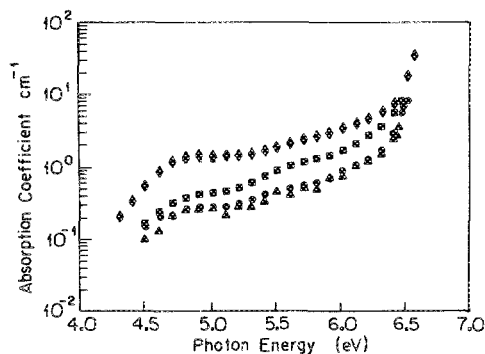


FIG. 1. UV absorption results for YAGs I-IV. The absorption coefficient  $\alpha$ , in  $\text{cm}^{-1}$ , is plotted vs photon energy in eV. YAG I results are represented by the squares, YAG II by the circles, YAG III by the diamonds, and YAG IV by the triangles.

samples. No changes in the spectrophotometer transmission characteristics were detected.

Figure 1 shows a plot of the UV absorption results for YAGs I-IV. The absorption coefficient  $\alpha$ , in  $\text{cm}^{-1}$ , is plotted versus photon energy in eV. YAG I results are represented by the squares, YAG II by the circles, YAG III by the diamonds, and YAG IV by the triangles. As can be seen from the figure, there is a considerable variability in absorption coefficient among the different YAG crystals. In another absorption study on multiple pieces of undoped YAG, Slack *et al.*<sup>9</sup> showed the same sort of variation in optical absorption coefficient in the 4.5- to 6.5-eV range. Two of the boules which luminesce yellow-green, YAGs II and IV, have the smallest absorption throughout the measurement range. From this, it is evident that the yellow-green luminescence did not adversely effect the absorption of YAGs II and IV in this region as compared to the absorption in YAG I, which did not exhibit the luminescence. At 6.5 eV, the YAG I-IV curves merge together and increase in absorption as they track the onset of the UV absorption edge. This energy was reported by Slack *et al.*<sup>9</sup> to be the start of the fundamental absorption in undoped YAG.

In Fig. 1, there is one absorption band that is readily discernable from all four curves. This is the feature that is centered at approximately 4.8 eV. This absorption was previously seen by Slack *et al.*<sup>9</sup> and Devor and co-workers.<sup>14</sup> This feature has been identified as a charge transfer band due to  $\text{Fe}^{3+}$ .<sup>26</sup> In recent optical and electron paramagnetic resonance studies, Chen *et al.*<sup>27</sup> have attributed the 4.8 eV charge transfer band to  $\text{Fe}^{3+}$  substituting for Al at both tetrahedral and octahedral lattice sites. In the present study, YAGs I and III have the largest concentrations of Fe and exhibit the largest 4.8-eV absorptions. Although the results of the SSMS analyses indicate that the Fe concentrations are comparable in YAGs I and III, there is a factor of 4 difference in the absorption coefficient at 4.8 eV. This effect may be due to differences in the actual Fe concentrations. For trace impurity concentrations in  $\text{Al}(\text{OH})_3$  powder, Tebbe *et al.*<sup>28</sup> have found chemical analyses from Northern Analytical Laboratory to be within a factor of 2 of known impurity concentrations for 65% of the analyses

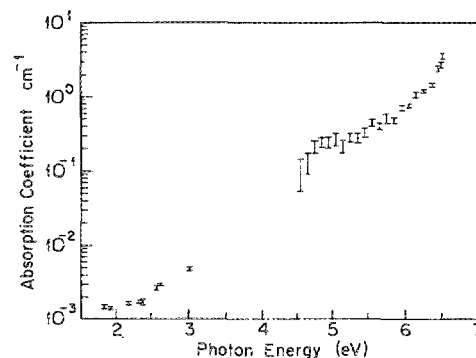


FIG. 2. UV and calorimetric absorption results for YAG IV. The calorimetry is the data in the 1.5- to 3.5-eV range. The YAG IV UV results are the same as depicted in Fig. 1 except that they are shown in Fig. 2 with error bars. All error bars in the figure are computed at one standard deviation.

and within a factor of 3 for 85% of the analyses. For example, samples with known concentrations of Fe have been analyzed to contain 50% of the actual Fe concentration.

The only other feature present in the YAG crystals is a less prominent absorption centered at 5.6 eV. Absorption in the vicinity of 5.6 eV has been linked to the presence of  $\text{Ce}^{3+}$  and an intrinsic lattice defect by Wong and co-workers<sup>11</sup> and to the presence of  $\text{Nd}^{3+}$  by Rooze and Anisimov.<sup>10</sup> The 5.6-eV feature is most pronounced in YAG I. According to the chemical analysis of Table II, YAG I contains both Ce and Nd, although Nd is detected close to the sensitivity limit for that analysis.

The next figure, Fig. 2, shows UV and calorimetric absorption results for YAG IV. The YAG IV UV results are the same as depicted in Fig. 1 except that they are shown in Fig. 2 with the appropriate error bars. These error bars and the error bars for the calorimetric measurements are computed at one standard deviation. The calorimetry, which is the data in the 1.5- to 3.5-eV energy range, is total absorption data on a 1.1-cm sample; it has not been separated into surface and bulk absorption. Hence, the calorimetry should be viewed as an upper bound for the value of the bulk absorption coefficient in this region. It is interesting to note that the calorimetric absorption results appear to level off at  $1.5 \times 10^{-3} \text{ cm}^{-1}$  for energies less than 2.0 eV. It is also interesting that the calorimetric results suggest a lower visible region absorption than that measured by Devor and co-workers<sup>14</sup> using relative transmission on as-grown undoped YAG. The difference between the two estimates of the bulk absorption coefficient is greater than an order of magnitude through the visible range.<sup>29</sup>

From the combination of UV and calorimetric measurements, a simple empirical relation can be written to obtain an approximate value for the absorption coefficient of undoped YAG over three decades of magnitude ( $1.0 \times 10^{-3}$  to  $1.0 \text{ cm}^{-1}$ ). This empirical relation can be employed as an order of magnitude estimate of the optical absorption coefficient. It is written as

$$\alpha = 10^{-4.5} \text{ cm}^{-1} \times 10^{E[\text{eV}]/1.3} \text{ eV}, \quad (1)$$

where  $\alpha$  is the absorption coefficient in  $\text{cm}^{-1}$  and  $E$  is the photon energy in eV. Equation (1) is applicable in the energy range from 2.3 to 6.4 eV and for the range of  $\alpha$  mentioned above. An empirical relation for absorption in Nd:YAG was previously published by Gorban, Gumenyuk, and Degoda,<sup>30</sup> but it covers a much narrower range of energy (4.1 to 6.2 eV) as compared to the present relation. Since no temperature-dependent studies of optical absorption were performed, an Urbach<sup>31,32</sup> model was not assumed for the absorption coefficient.

## V. CONCLUSION

In this work, UV absorption spectra on four boules of undoped Cz-grown optical quality YAG have been obtained. From the UV spectra (Fig. 1), it is observed that the four boules of undoped YAG are as much as an order of magnitude different in optical absorption coefficient in the 4.5- to 6.4-eV range. The optical absorption of YAG in this energy range is greatly influenced by extrinsic mechanisms, i.e., impurities. The results from the present study show two pronounced absorption features: one at 4.8 eV due to  $\text{Fe}^{3+}$ , and the other at 5.6 eV which can be partially attributed to trace impurity concentrations.

In addition to the UV measurements, calorimetric measurements were performed on one of the YAG boules to estimate the bulk absorption coefficient in the visible and near-IR regions. The calorimetric measurements suggest a leveling off of the optical absorption of undoped YAG in the red and near IR at a value of  $1.5 \times 10^{-3} \text{ cm}^{-1}$ . From the combination of UV and calorimetric measurements, a simple empirical relation has been written to obtain an approximate value for the absorption coefficient of undoped YAG over three decades of magnitude,  $1.0 \times 10^{-3}$  to  $1.0 \text{ cm}^{-1}$ .

## ACKNOWLEDGMENTS

We are extremely grateful to Mr. Ralph Eno of Hamamatsu Corporation for a generous gift of equipment. We would like to thank C. L. Fincher of The Aerospace Corporation for help with the luminescence measurements. Thanks are also in order for use of the facilities at The Aerospace Corporation for processing of the YAG boules. We would like to thank Professor M. Birnbaum of the Center for Laser Studies, University of Southern California for supplying one of the YAG boules. In addition, we are indebted to Laser Power Optics for their expert polishing of the samples. One of the authors, MEI, wishes to thank Phi Kappa Phi and Rockwell International for fellowship support.

- <sup>1</sup> H. S. Yoder and M. L. Keith, *Am. Mineral.* **36**, 519 (1951).
- <sup>2</sup> Z. L. Kiss and R. J. Pressley, *Appl. Opt.* **5**, 1474 (1966).
- <sup>3</sup> G. Menzer, *Z. Krist.* **69**, 300 (1929).
- <sup>4</sup> J. E. Geusic, H. M. Marcos, and L. G. Van Uitert, *Appl. Phys. Lett.* **4**, 182 (1964).
- <sup>5</sup> G. Blasse and A. Bril, *Appl. Phys. Lett.* **11**, 53 (1967).
- <sup>6</sup> D. J. Robbins, B. Cockayne, B. Lent, and J. L. Glasper, *J. Electrochem. Soc.* **126**, 1556 (1979).
- <sup>7</sup> H. M. O'Bryan and P. B. O'Conner, *J. Am. Ceram. Soc.* **45**, 578 (1966).
- <sup>8</sup> M. Bass and A. E. Paladino, *J. Appl. Phys.* **38**, 2706 (1967).
- <sup>9</sup> G. A. Slack, D. W. Oliver, R. M. Chrenko, and S. Roberts, *Phys. Rev.* **177**, 1308 (1969).
- <sup>10</sup> N. S. Rooze and M. A. Anisimov, *Opt. Spect.* **38**, 356 (1975).
- <sup>11</sup> C. M. Wong, S. R. Rotman, and C. Warde, *Appl. Phys. Lett.* **44**, 1038 (1984).
- <sup>12</sup> T. Tomiki, F. Fukudome, M. Kaminao, M. Fujisawa, and Y. Kaminao, *J. Phys. Soc. Jpn.* **55**, 2090 (1986).
- <sup>13</sup> T. Tomiki, J. Tamashiro, M. Hiraoka, N. Hirata, and T. Futemma, *J. Phys. Soc. Jpn.* **57**, 4429 (1988).
- <sup>14</sup> D. P. Devor, R. C. Pastor, and L. G. DeShazer, *J. Chem. Phys.* **81**, 4104 (1984).
- <sup>15</sup> M. E. Innocenzi, R. T. Swimm, M. Bass, R. H. French, A. B. Villaverde, and M. R. Kokta, *J. Appl. Phys.* **67**, 7542 (1990).
- <sup>16</sup> M. E. Innocenzi, Ph.D. thesis, USC, Los Angeles, CA, 1989, available from University Microfiche, Ann Arbor, MI.
- <sup>17</sup> The stated purity of the starting materials is based on the total cation impurity content by weight. For example, a 4 9's purity  $\text{Y}_2\text{O}_3$  powder should contain 999.9 g of pure  $\text{Y}_2\text{O}_3$  and no more than 0.1 g of all cation impurities per 1000 g of powder. For the 4 9's case, this would be equivalent to a cation impurity content of no more than 100 ppmw, where ppmw is parts per million by weight.
- <sup>18</sup> Northern Analytical Laboratory, Inc., Amherst, NH.
- <sup>19</sup> Laser Power Optics, 12777 High Bluff Dr., San Diego, CA.
- <sup>20</sup> The Aerospace Corporation, P.O. Box 92957, Los Angeles, CA.
- <sup>21</sup> H. J. Bernhardt, *Phys. Status Solidi* **31**, 365 (1975).
- <sup>22</sup> D. J. Robbins, B. Cockayne, B. Lent, C. M. Duckworth, and J. L. Glasper, *Phys. Rev. B* **19**, 1254 (1979).
- <sup>23</sup> S. R. Rotman and C. Warde, *J. Appl. Phys.* **58**, 522 (1985).
- <sup>24</sup> S. R. Rotman, R. P. Tandon, and H. L. Tuller, *J. Appl. Phys.* **57**, 1951 (1985).
- <sup>25</sup> S. R. Rotman and H. L. Tuller, *J. Appl. Phys.* **62**, 1305 (1987).
- <sup>26</sup> M. L. Meil'man, M. V. Korzhik, V. V. Kuz'min, M. G. Livshits, Kh. S. Bagdasarov, and A. M. Kevorkov, *Sov. Phys. Dokl.* **29**, 61 (1984).
- <sup>27</sup> C. Y. Chen, G. J. Pogatschnik, Y. Chen, and M. R. Kokta, *Phys. Rev. B* **38**, 8555 (1988).
- <sup>28</sup> F. N. Tebbe, P. A. Morris, R. H. French, U. Chowdhry, and R. L. Coble, *J. Am. Ceram. Soc.* **71**, C-204 (1988).
- <sup>29</sup> Although the exact values of Devor's visible absorption results after postgrowth processing are impossible to discern, they appear to be more in agreement with this study's as-grown results. This is not unreasonable since Union Carbide utilizes a patented process to remove OH contamination (hydration) from the starting materials before the growth of their YAG. Devor's postgrowth processing also removes OH contamination, thereby reducing the bulk absorption in the visible region.
- <sup>30</sup> I. S. Gorban, A. F. Gumenyuk, and V. Ya. Degoda, *Opt. Spect. (USSR)* **58**, 428 (1985).
- <sup>31</sup> F. Urbach, *Phys. Rev.* **92**, 1324 (1953).
- <sup>32</sup> J. D. Dow and D. Redfield, *Phys. Rev. B* **5**, 594 (1972).